 CMES, vol.3, no.4, pp.465-481, 2002

Temperature Distributions and Thermoelastic Displacements In Moving Bodies

Shuangbiao Liu, Michael J. Rodgers, Qian Wang, Leon M. Keer, and Herbert S. Cheng[1]

Abstract: Computing the temperature rise and thermoelastic displacement of a material subjected to frictional heating is essential for the realistic modeling of the performance of mechanical components. This paper presents a novel set of frequency-domain expressions for the surface temperature rise and the surface normal thermoelastic displacement of a moving three-dimensional elastic halfspace subjected to arbitrary transient frictional heating, where the velocity of the body and its direction can be an arbitrary function of time. Frequency response functions are derived by using the Carslaw-Jaeger theory, the Seo-Mura result, and the Fourier transform. General formulas are expressed in the form of time integrals, and important expressions for constant body motion velocities are given for the transient-instantaneous, transient-continuous, and steady-state cases. The thermoelastic responses, in terms of temperature rise and thermoelastic displacement, of the halfspace surface in configurations similar to pin-on-disk contacts are simulated and discussed.

Nomenclature

d_j	$\int_{t'}^{t} Pe_j(\tau)d\tau/\Delta t$
$\mathrm{erf}(x)$	error function, $\frac{2}{\sqrt{\pi}}\int_0^x \exp(-\tau^2)d\tau$
$\mathrm{erfc}(x)$	complementary error function, $\frac{2}{\sqrt{\pi}}\int_x^\infty \exp(-\tau^2)d\tau$
i	pure imaginary, $\sqrt{-1}$
K	conductivity, J/m $^\circ$ ks or w/m $^\circ$ k
l	characteristic length, m
Pe_j	Péclet number, $\overline{V}_j l/\kappa$
$\overline{q}$	heat source, W/m^2 or N/ms
q	non-dimensional heat source, $\overline{q}\alpha_t l/K$
$\overline{T}$	temperature rise, $^\circ$ k
T	non-dimensional temperature rise, $T=\alpha_t\overline{T}$
$\overline{t}$	time, s
t	non-dimensional time, $\kappa\overline{t}/l^2$
$\overline{u}_j$	thermoelastic displacement, m
u_j	non-dimensional thermoelastic displacement field, $\overline{u}_j/[l(1+\nu)]$
$\overline{V}_j$	velocity in the x_j direction, m/s
w	frequency domain radius, $\sqrt{\omega_1^2+\omega_2^2}$
w'	effective frequency domain radius, $\sqrt{w^2+\mathrm{i}(\omega_1 d_1+\omega_2 d_2)}$
$\overline{x}_j$	coordinate, m
x_j	non-dimensional coordinate in j direction, $\overline{x}_j/l$
α_t	linear thermal expansion coefficient, m/m $^\circ$ k
δ_{ij}	Kronecker delta
Δt	$t-t'$
κ	thermal diffusivity, m^2/s
ν	Poisson's ratio
ω_1,ω_2	frequency domain counterparts of x_1, x_2, respectively
ω_t	counterpart of time in the frequency domain
$(\ )_{,j}$	partial derivative with respect to x_j coordinate
$\tilde{}$	each Fourier Transform

1 Introduction

Frictional heating has been an engineering research topic with a long history. Controlling the effects arising from frictional heating has been a vital part of mechanical engineering design. With the development and constant improvement of computer modeling capabilities, researchers have been able to perform detailed modeling and simulation of frictional heating and contact. Tribological simulations of frictional heating effects include studies on flash temperature [Tian and Kennedy 1994, Qiu and Cheng 1998, and Gao et al. 2000], thermoelastic displacement [Ling and Mow 1965, Barber 1972, Barber 1984, Barber 1987, and Liu et al. 2001], thermoelastic fields [Ju and Chen 1984, Huang and Ju 1985, Bryant

[1] Center for Surface Engineering and Tribology; Northwestern University; Evanston, IL 60208, USA; 847-467-6961; 847-467-3427 (fax); liusb@northwestern.edu

1988, Leroy et al. 1989, Leroy et al. 1990, Ju and Farris 1997, Mow and Cheng 1967, and Ting and Winer 1989], thermoelastic contact [Azarkhin and Barber 1987, Yevtushenko and Kulchytsky-Zhyhailo 1995a, Yevtushenko and Kulchytsky-Zhyhailo 199b, Wang and Liu 1999, Liu and Wang 2000, and Liu and Wang 2001], and thermoelastic instability [Barber 1969, Dow and Burton 1972, Yi et al 1999]. Most of this research is based on the knowledge of heat conduction that is thoroughly and systematically presented by Carslaw and Jaeger's [Carslaw and Jaeger 1959] (see also [Ling 1973 and Johnson 1996]).

A new approach for calculating the thermoelastic displacement on the surface of an elastic halfspace has been recently developed [Liu et al. 2001], which treats the temperature field as an inclusion. Halfspace problems, which are particularly important to Tribology, are solved by using Seo-Mura inclusion theory. Expressions were developed for the thermoelastic displacement in transient-instantaneous, transient-continuous (time-invariant heat source), and steady-state cases. Frequency response functions (FRFs) for the surface normal thermoelastic displacement were solved [Liu et al. 2001] by substituting the temperature field [Carslaw and Jaeger 1959] into the inclusion formula [Seo and Mura 1979], changing the order of integration and applying the Fourier transform and convolution theorem [Press et al. 1992 and Morrison 1997]. These frequency response functions are useful in simulations with arbitrary input because of the recently developed algorithm that uses the fast Fourier transform (FFT) to convert frequency response functions into influence coefficients and uses discrete convolution and fast Fourier transform (DC-FFT) method to determine the material response [Liu et al. 2000 and Liu and Wang 2002].

In this paper, the new analytical approach [Liu et al. 2001] is extended to obtain a novel set of frequency response functions for the surface temperature rise and the surface thermoelastic displacement in moving three-dimensional (3D) elastic halfspace (the coordinate system is fixed to the heat source) subjected to arbitrary transient frictional heating, where the velocity and its direction of the body can be an arbitrary function of time. General formulas are expressed in the form of a time integral, and important expressions are given for the transient-instantaneous, transient-continuous, and steady-state cases. The new formulas allow the fast Fourier transform to be conveniently used to calculate the thermoelastic responses directly from the applied heat source. As examples, the new formulas are applied to simulate the thermoelastic response of a halfspace with similar configurations as in pin-on-disk experiments.

2 Problem Description

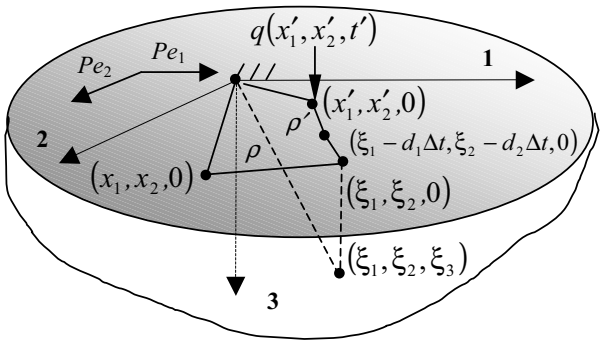

Figure 1 : Description of the physcial domain and coordinates

A halfspace (Fig. 1) of a uniform initial temperature distribution is subject to a heat source on the surface. A non-dimensional coordinate system $x_j = \bar{x}_j / l$ with characteristic length l is fixed to the heat source, and the halfspace is moving relative to the heat source and the coordinate system along the x_j coordinate with speeds ($\overline{V}_1$, $\overline{V}_2$, and $\overline{V}_3 \equiv 0$), which can be functions of time but not space. The material properties of the halfspace are the diffusivity (κ), the linear thermal expansion coefficient (α_t), the Poisson's ratio (ν), and the conductivity (K). The heat source causes a non-dimensional temperature rise $T = \alpha_t \overline{T}$ in the halfspace, resulting in a non-dimensional thermoelastic displacement, $u_j = (\vec{x}, t) = \overline{u}_j(\vec{x}, t)/[l(1+\nu)]$, in the x_j coordinate direction. The uncoupled governing partial differential equations for transient heat conduction and quasistatic thermoelastic deformation are as follows:

$$T_{,ii} = \frac{\partial T}{\partial t} + Pe_1 T_{,1} + Pe_2 T_{,2} \tag{1}$$

$$u_{i,jj} + u_{j,ji} / (1-2\nu) = 2T_{,i} / (1-2\nu) \tag{2}$$

where t is the non-dimensional time, $t = \kappa \bar{t} / l^2$; Pe_j is the Péclet number in the x_j direction, $Pe_j = \overline{V}_j l / \kappa$; Roman

indices range over 1, 2, 3; the summation convention is assumed; and $(\ )_{,j} = \frac{\partial(\ )}{\partial x_j}$. The temperature and thermoelastic boundary conditions for the surface are

Thermal BC:

$$-T_{,3} = q \tag{3}$$

Traction free BC:

$$(1-2\nu)(u_{3,j}+u_{j,3}) + 2\nu\delta_{3j}u_{k,k} = 2\delta_{3j}T \tag{4}$$

where the non-dimensional heat source is defined as $q(x_1,x_2,t) = \overline{q}\alpha_t l/K$ for $t \geq 0$, and $q(x_1,x_2,t) \equiv 0$ for $t < 0$. The traction-free boundary condition allows the thermoelastic analysis in this paper to be directly superposed with an isothermal elastic contact analysis [Liu and Wang 2001].

As the heat source may vary with respect to time, the thermoelastic problem may be discussed in three cases accordingly [Barber 1972]: the transient-instantaneous case with a position and time dependent heat source, $q(x_1,x_2,t)$ and arbitrary time, the transient-continuous case with position dependent heat source, $q(x_1,x_2)$ and arbitrary time, and the steady-state case with position dependent heat source, $q(x_1,x_2)$ and $t \to \infty$. Solutions to these heat-source conditions in a moving body offer a general formulation set for the frictional-heating problems.

3 Distribution of Temperature Rise

The solution of Eqs. (1) and (3) for the temperature rise caused by the surface heat source, $q(x_1',x_2',t')$, can be expressed as follows [Carslaw and Jaeger 1959]:

$$T(\xi_1,\xi_2,\xi_3,t) =$$

$$\frac{1}{4\pi^{3/2}}\int_0^t\int_{-\infty}^{+\infty}\int_{-\infty}^{+\infty} q(x_1',x_2',t')\frac{e^{-\frac{\rho'^2+\xi_3^2}{4\Delta t}}}{\Delta t^{3/2}}dx_1'dx_2'dt' \tag{5a}$$

where $\Delta t = t - t'$, the effective velocities are $d_j = \int_{t'}^{t} Pe_j(\tau)d\tau/\Delta t$, and $\rho'^2 = (\xi_1 - x_1' - d_1\Delta t)^2 + (\xi_2 - x_2' - d_2\Delta t)^2$ (Fig. 1). Equation (5a) can also be written in a convolution form,

$$T(\xi_1,\xi_2,\xi_3,t) = \int_0^t q(\xi_1,\xi_2,t') **G(\xi_1,\xi_2,t,t')dt' \tag{5b}$$

with the Green's function,

$G(\xi_1,\xi_2,\xi_3,t,t') = \frac{1}{4(\Delta t\pi)^{3/2}}\exp[-\frac{(\xi_1-d_1\Delta t)^2+(\xi_2-d_2\Delta t)^2+\xi_3^2}{4\Delta t}]$.

The symbol '**' stands for a two-dimensional (2D) convolution. Applying the 2D Fourier transform (FT) with respect to the ξ_1 and ξ_2 directions, Eqs. (A3) and (A5), and the convolution theorem (Appendix A), a general form of the temperature rise in a hybrid domain (frequency, depth and time) is expressed as time dependent integral,

$$\tilde{\tilde{T}}(\omega_1,\omega_2,\xi_3,t) = \frac{1}{\sqrt{\pi}}\int_0^t \tilde{\tilde{q}}(\omega_1,\omega_2,t')\frac{1}{\sqrt{\Delta t}}\exp(-\frac{\xi_3^2}{4\Delta t} - \Delta t w'^2)\,dt' \tag{6}$$

Variables ω_1 and ω_2 are the angular frequencies in the frequency domain; and a double tilde ($\tilde{\tilde{}}$) implies a 2D Fourier transform. The frequency domain radius is $w = \sqrt{\omega_1^2+\omega_2^2}$, and the effective frequency domain radius is $w' = \sqrt{w^2 + \mathrm{i}(\omega_1 d_1 + \omega_2 d_2)}$. If the Péclet numbers (or velocities, $\overline{V}_1$ and $\overline{V}_2$) vary with time, numerical integration must be used for the effective velocities d_j and for Eq. (6) to evaluate the time integrals. In the following, important formulas with time-invariant Péclet numbers, i.e., $d_j = Pe_j$= constant, are discussed.

Transient-Instantaneous Case. Since the heat source $\tilde{\tilde{q}}(\omega_1,\omega_2,t)$ and the function $\tilde{\tilde{g}}(\omega_1,\omega_2,\xi_3,t) = \exp(-\frac{\xi_3^2}{4t} - tw'^2)\Big/\sqrt{\pi t}$ are zero when $t < 0$, Eq. (6) is a convolution related to the Fourier transform with respect to t, and can be expressed as (see Eq. (A8))

$$\frac{\tilde{\tilde{\tilde{T}}}(\omega_1,\omega_2,\xi_3,\omega_t)}{\tilde{\tilde{\tilde{q}}}(\omega_1,\omega_2,\omega_t)} = \frac{\exp(-\xi_3\sqrt{w'^2+\mathrm{i}\omega_t})}{\sqrt{w'^2+\mathrm{i}\omega_t}} \tag{7}$$

where ω_t is the frequency domain counterpart of time, and a triple tilde ($\tilde{\tilde{\tilde{}}}$) implies a 3D Fourier transform. The right-hand side of Eq. (7) is the corresponding frequency response function (FRF) for transient-instantaneous temperature rise, which gives the temperature rise caused by an instantaneous point heat source.

Transient-Continuous Case. If the heat source is not a function of time, Eq. (6) can be written as

$$\tilde{\tilde{T}}(\omega_1,\omega_2,\xi_3,t) = \frac{\tilde{\tilde{q}}(\omega_1,\omega_2)}{\sqrt{\pi}}\int_0^{\sqrt{t}} 2\exp(-\frac{\xi_3^2}{4\tau^2} - \tau^2 w'^2)d\tau \tag{8}$$

with $\tau = \sqrt{\Delta t}$. Therefore,

$$\frac{\tilde{\tilde{T}}(\omega_1,\omega_2,\xi_3,t)}{\tilde{\tilde{q}}(\omega_1,\omega_2)} = \begin{cases} w'\neq 0 \\ \left[e^{-\xi_3 w'}\mathrm{erfc}(\frac{\xi_3}{2\sqrt{t}} - w'\sqrt{t}) - e^{\xi_3 w'}\mathrm{erfc}(\frac{\xi_3}{2\sqrt{t}} + w'\sqrt{t})\right]/(2w') \\ w'=0 \\ \left[2\exp(-\frac{\xi_3^2}{4t}\sqrt{t}/\sqrt{\pi} - \xi_3]\mathrm{erfc}(\frac{\xi_3}{2\sqrt{t}})\right] \end{cases} \quad (9)$$

The right-hand side of Eq. (9) is the frequency response function for transient-continuous temperature rise, which gives the temperature rise caused by a continuous point heat source. If the velocities are not zero, Eq. (9) includes a complementary error function $\mathrm{erfc}(x)$ with complex arguments and can be evaluated by using a special function, $\varpi(z)$ [Abramowitz and Stegun 1964, Appendix B]. The solution in Ting and Winer's paper [1989] is a stationary case of Eq. (9).

Steady-State Case. The frequency response function for steady-state temperature rise is found from Eq. (7) by letting $\omega_t = 0$, or from Eq. (9) by letting $t \to \infty$,

$$\frac{\tilde{\tilde{T}}(\omega_1,\omega_2,\xi_3)}{\tilde{\tilde{q}}(\omega_1,\omega_2)} = \frac{e^{-\xi_3 w'}}{w'} \quad (10)$$

Again, note that Eqs. (7), (9 and (10) are only valid for constant Péclet numbers (velocities).

4 Normal Surface Thermoelastic Displacement

The solution of Eqs. (2) and (4) for the quasi-static thermoelastic displacement is found from the Green's function for a point force in the interior of a halfspace [Mindlin 1953], using the approach of Seo and Mura [1979]. The normal surface thermoelastic displacement is given by [Liu et al. 2001]

$$u_3(x_1,x_2,0,t) = \frac{-1}{\pi} \int_0^{+\infty}\int_{-\infty}^{+\infty}\int_{-\infty}^{+\infty} T(\xi_1,\xi_2,\xi_3,t)\frac{\xi_3}{(\rho^2+\xi_3^2)^{3/2}} d\xi_1 d\xi_2 d\xi_3 \quad (11)$$

where $\rho^2 = (x_1-\xi_1)^2 + (x_2-\xi_2)^2$. Similar to Equations (5), the convolution theorem and Eq. (A6) are used to take the 2D Fourier transform of Eq. (11), giving

$$\tilde{\tilde{u}}_3(\omega_1,\omega_2,0,t) = -2\int_0^{+\infty} \tilde{\tilde{T}}(\omega_1,\omega_2,\xi_3,t)\exp(-\xi_3 w)\, d\xi_3 \quad (12)$$

Substituting Eq. (6) into Eq. (12) gives

$$\tilde{\tilde{u}}_3(\omega_1,\omega_2,0,t) = \frac{-2}{\sqrt{\pi}} \int_0^{+\infty}\int_0^t \tilde{\tilde{q}}(\omega_1,\omega_2,t')\frac{1}{\sqrt{\Delta t}}\exp\left(\frac{\xi_3^2}{4\Delta t} - \Delta t w'^2 - \xi_3 w\right) dt' d\xi_3 \quad (13)$$

Interchanging the order of integration allows the depth integral to be performed analytically, resulting in the following compact form

$$\tilde{\tilde{u}}_3(\omega_1,\omega_2,0,t) = -2 \int_0^t \tilde{\tilde{q}}(\omega_1,\omega_2,t')\exp[-\mathrm{i}\Delta t(\omega_1 d_1 + \omega_2 d_2)]\mathrm{erfc}(w\sqrt{\Delta t})\, dt' \quad (14)$$

which is the general form of the normal surface thermoelastic displacement expressed in a hybrid domain (frequency and time). If the Péclet numbers vary with time, numerical integration must be used to evaluate the time integrals for the effective velocities d_j and for Eq. (14). However, important formulas with constant Péclet numbers are further discussed below.

Transient-Instantaneous Case. For the transient-instantaneous case with constant Péclet numbers, Eq. (14) is treated as a convolution related to the Fourier transform with respect to t. Applying the convolution theorem, the frequency-shift property of the Fourier transform, and Eq. (A7) gives

$$\frac{\tilde{\tilde{u}}_3(\omega_1,\omega_2,0,\omega_t)}{\tilde{\tilde{q}}(\omega_1,\omega_2,\omega_t)} = \frac{-2}{\sqrt{\mathrm{i}\omega_t + w'^2}\,(\sqrt{\mathrm{i}\omega_t + w'^2} + w)} \quad (15)$$

Therefore, the corresponding frequency response function, which gives the displacement caused by an instantaneous heat source, is given by the right-hand-side of Eq. (15) with a singularity when both w = 0 and ω_t = 0 (note that w' = 0 when w = 0).

Transient-Continuous Case. If the Péclet numbers are constant and the heat source is not a function of time, Eq. (14) is written as

$$\tilde{\tilde{u}}_3(\omega_1,\omega_2,0,t) = -2\tilde{\tilde{q}}(\omega_1,\omega_2) \int_0^t \exp[-\mathrm{i}(\omega_1 d_1+\omega_2 d_2)\tau]\,\mathrm{erfc}\left(w\sqrt{\tau}\right)\, d\tau \qquad (16)$$

Equation (16) is integrated, and the frequency response function for the transient-continuous case is given by the right-hand-side of

$$\frac{\tilde{\tilde{u}}_3(\omega_1,\omega_2,0,t)}{\tilde{\tilde{q}}(\omega_1,\omega_2)} = 2\mathrm{i}\{1-\exp[-(\omega_1 d_1+\omega_2 d_2)\mathrm{i}t]\mathrm{erfc}(w\sqrt{t}) - w\,\mathrm{erf}(w'\sqrt{t})/w'\}\Big/(\omega_1 d_1+\omega_2 d_2) \qquad (17)$$

The frequency response function gives the displacement caused by a continuous heat source. When the velocities are zero, Eq. (17) does not apply; instead, Eq. (16) should be integrated for that case (the result is given in [Liu et al. 2001]). At w = 0, the frequency response function is '$-2t$', and therefore it has no singularity. The frequency response function includes an error function $\mathrm{erf}(x)$ with complex arguments, which again can be evaluated by using the special function $\varpi(z)$ [Abramowitz and Stegun 1964, Appendix B].

Steady-State case. When steady-state conditions prevail, Eq. (16) is integrated analytically, and the frequency response function for the steady-state case is given by the right-hand-side of

$$\frac{\tilde{\tilde{u}}_3(\omega_1,\omega_2,0)}{\tilde{\tilde{q}}(\omega_1,\omega_2)} = \frac{-2}{w'\,(w'+w)} \qquad (18)$$

which is a special case of the transient frequency response function from Eq. (15) with $\omega_t = 0$, and has a singularity at w = 0. One of the striking properties of frequency response functions is that the frequency response functions in a plane-strain problem are simply those in a three-dimensional problem with ω_2 = 0 [Liu and Wang 2002]. Equation (18) with $\omega_2 = 0$ agrees with the 2D result obtained by Bryant [1988] or Ju and Farris [1997]. Note that Eqs. (15 – 18) again are valid only for constant Péclet numbers. If the speeds are zero, the expressions in Eqs. (14 - 18) reduce to the results given by [Liu et al. 2001]. It should be pointed out that the entire thermoelastic displacements at any interior location of the halfspace could be obtained following the same derivation process.

5 Numerical Methods

For problems with an irregular heat source, the discrete convolution and fast Fourier transform algorithm [Liu and Wang 2002] may be used to obtain efficient and accurate results. The influence coefficients [Johnson 1996] of the responses (temperature rise and normal surface thermoelastic displacement) are essential in this algorithm. If the heat source has a known Fourier transform, the responses can be obtained from Eqs. (6), (7), (9) or (10) and Eqs. (14), (15), (17) or (18) by inverse Fourier transform, which could be numerically calculated in several ways. In this paper, the conversion process [Liu and Wang 2002] with inverse fast Fourier transform (FFT) algorithm is used, which is an essential part to obtain the influence coefficients in the discrete convolution and fast Fourier transform algorithm. Given the intervals (Δ_1 and $\Delta_2$for x_1 and x_2 directions) in the space domain, frequency response functions are truncated between negative and positive Nyquist frequencies ($\pm\pi/\Delta_1$ and $\pm\pi/\Delta_2$ for ω_1 and ω_2 directions). If the space and frequency domains have the same number of discrete points (N_1 and N_2 for x_1 and x_2 directions, and for ω_1 and ω_2 directions), the aliasing error in the results obtained by the conversion process may become significant. In order to reduce the aliasing error, the number of discrete points in the frequency domain should be large enough. In this paper, the number of discrete points in the frequency domain are $8N_1$ and $8N_2$ in the ω_1 and ω_2 directions, respectively, and this choice has the effect of refining the interval in the frequency domain for sufficiently accurate results.

Since the complementary error function and error function require a significant amount of computation, the following approximations are used to save computation time, $\mathrm{erfc}(x \geq 3) = 0, \quad \mathrm{erf}(x \geq 3) = 1$. Standard Gaussian quadrature is used to carry out the numerical integration in Eqs. (6) and (14), when numerical integration is necessary.

6 Numerical Simulations

The formulations developed in Sections 2-4 enable numerical simulation of the thermoelastic response of a

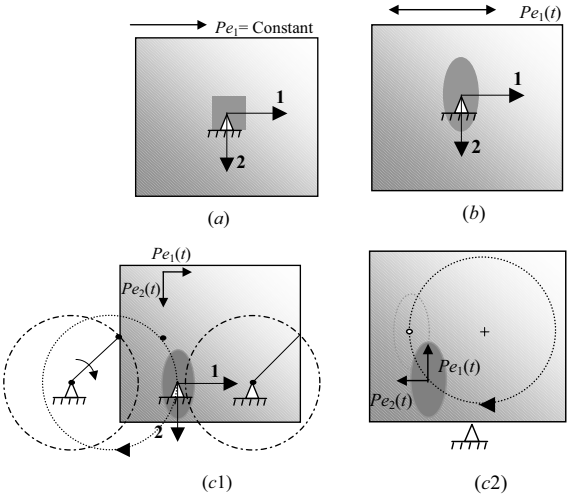

Figure 2 : Three translation motions of a halfspace (a) A rectangular heat source on a a pure translating halfspace. (b) An elliptical heat source on a reciprocating halfspace. (c1) An ellipitical heat source on a circularly translating halfspace. (c2) A circularly translating elliptical heat source on a fixed halfspace, which is equivalent to (c1).

halfspace by computing the transient three-dimensional temperature rise fields and normal surface thermoelastic displacement. Three example cases are numerically solved to illustrate the use of the formulations, where three different motions of the halfspace are specified to show the novelty of the formulations: pure translation (Fig. $2(a)$), reciprocating translation (Fig. $2(b)$), and circular translation (Fig. $2(c1)$). It should be pointed out that the three examples do not directly correspond to the three cases of heat source, and frequency response functions of Eqs. (7) and (15) for transient-instantaneous cases with a constant Péclet number are not exemplified in this paper. However, in pure translation, both transient-continuous and steady-state case are studied; in reciprocating translation, the transient-instantaneous case, which uses the general equations (6) and (14), is studied; in circular translation, the transient-continuous case is studied. In the latter two examples, the steady state results may not exist. In each simulation, a known heat source is given with regard to the coordinate system, which is fixed to the heat source. The values of velocities, characteristic lengths and material properties are chosen from a typical counterformal contact in tribological applications [Liu and Wang 2001]. Other parameters are chosen for the convenience. The temperature rise and the normal thermoelastic displacement are obtained on the surface discretzied with 128×128 rectangular elements, which is sufficient to give smooth results in all the cases studied. Note that the x_2 coordinates in Figs. 2 are downward to be consistent with Fig. 1. However, in all contour plots, x_2 are upward for the observation convenience. Also in all contours plots the interval between contours is fixed and the limits of axes are chosen to show results in a better focus. Although results are presented within only a single cycle for the latter two examples, it should be pointed out that the responses at any cycle or time could be calculated from the initial uniform state (nonuniform initial temperature condition is not explored in the current study) provided that the Gaussian integration is sufficiently accurate.

6.1 Pure Translation

Figure $2(a)$ describes the configuration with a constant heat source $q = 1$, over a region of $x_1 \in [-1/4, 1/4]$, $x_2 \in [-1/4, 1/4]$. The constant Péclet numbers are $Pe_1 = 10$, $Pe_2 = 0$, which correspond to $\overline{V}_1$=1 m/s and $\overline{V}_2$ = 0 m/s at l = 1 mm and κ=10^{-4} m^2/s. Results are computed in the region of $x_1 \in [-2, 2]$, $x_2 \in [-2, 2]$. The Nyquist critical angular frequencies in both directions are 32π. The temperature rise and the displacement are calculated with Eqs. (9 – 10) and with Eqs. (17 – 18), respectively. The results are plotted in Figs. 3 – 4 to show the evolution to steady state. Not surprisingly, the tails of both temperature and displacement distributions resemble wakes and spread outward perpendicular to the direction of motion and along the motion direction of the body. Because the temperature rise is directly related to the heat source, sharp temperature gradients appear around the border of the heat-application area, corresponding to the discontinuity of the heat source, as shown in Fig. 3. However, the temperature rise in the entire body causes the surface to deform, and the contours for the displacement distribution look smoother than those of the temperature rise, as shown in Fig. 4. Figures 5 and 6 further compare the responses along the line of $x_2 = 0$ at different times ($\bar{t}$=$0.01t$). The responses start from a nearly symmetric peak localized with respect to the region of the heat source application. Increasing the time of heating causes their peaks to rise due to the heat accumulation in the solid even though new parts of the surface continuously pass by the heat source. As a result of the halfspace

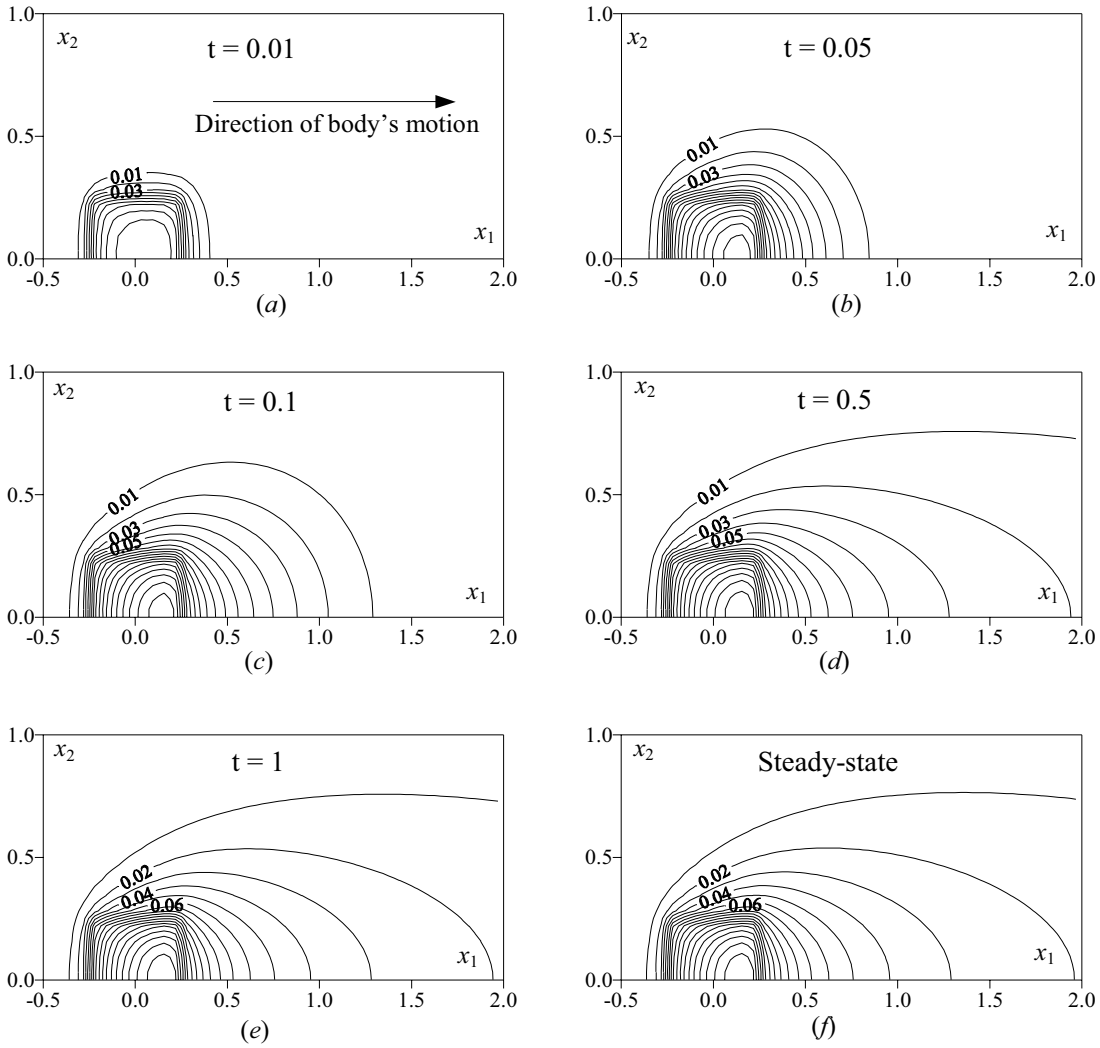

Figure 3 : Contours of the distributions of the surface temperature rise, $T(x_1, x_2, 0, t)$, of the purely translating halfspace (Fig. 2(a)). Here, (a) through (f) show the evolution as time increases, and (f) shows the stead-state case.

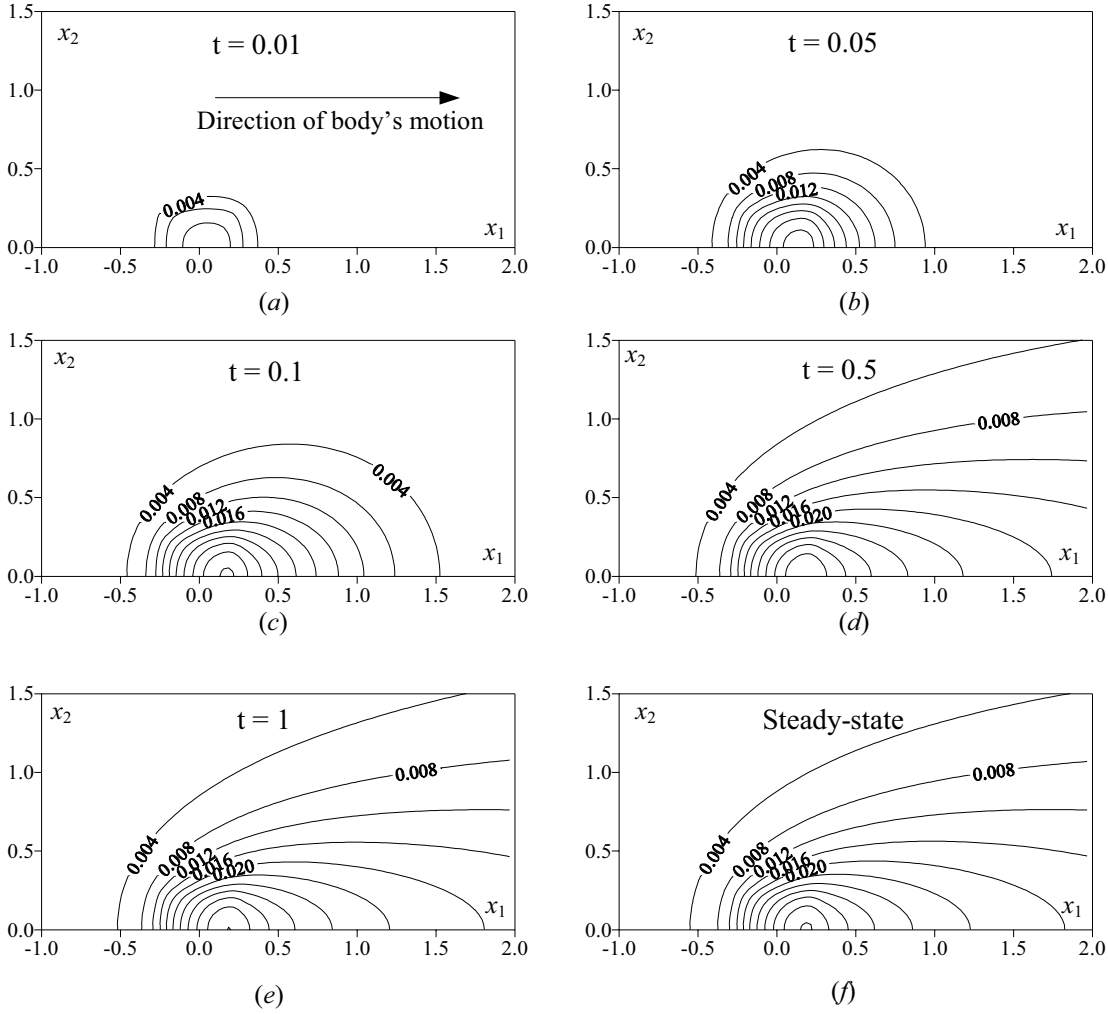

Figure 4 : Contours of the thermoelastic displacements, - $u_3(x_1, x_2, 0, t)$, of the pure translating halfspace (Fig. 2(a)). Pe_1 = 10, and Pe_2 = 0. Here, (a) through (f) show the evolution as time increases, and (f) shows the steady- state case.

translating to the positive direction of x_1, the responses in the positive side of x_1 becomes larger than those in the negative side of x_1. Therefore, the maximum values are found at positions in the positive side of the origin. The 2D steady state result corresponding to a heat source that has the same width of application as that of the 3D heat source used in this case is also calculated and shown in Fig. 5. The 2D steady-state temperature rise is higher than the 3D steady-state result because the heat source for the 2D solution is a line source (with the same width but with infinite length), and therefore the quantity of heat input is much higher for the 2D case.

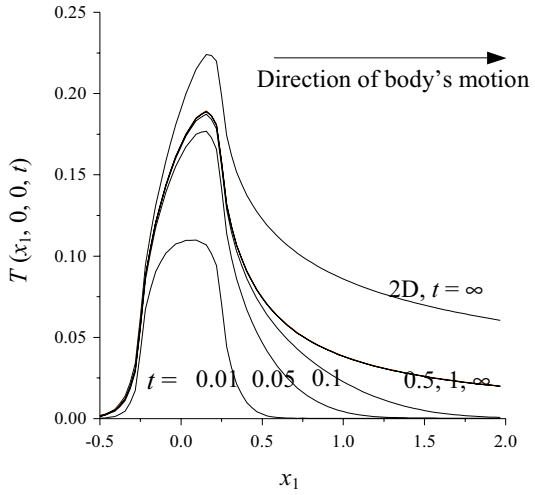

Figure 5 : Temperature rises on the surface of the halfspace under a pure translation motion at different times.

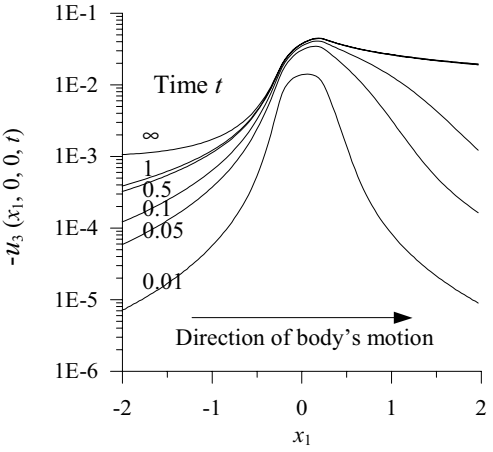

Figure 6 : Thermoelastic displacements of the surface of the halfspace under a pure translation motion at different times.

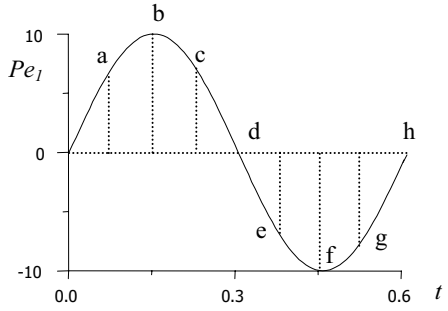

Figure 7 : Variation of the x-direction Péclet number for case B for the reciprocating halfspace.

6.2 Reciprocating Translation

Fig. 2(b) describes a reciprocating halfspace subjected to a stationary heat source that corresponds to the Hertzian pressure distribution $p = c\sqrt{1-(x_1/c_1)^2-(x_2/c_2)^2}$ with $c_1 = 0.25$, $c_2 = 0.5$, and $c = K/(\alpha_t \kappa)$, whose Fourier transform pairs is $2\pi c c_1 c_2(\sin\Theta - \Theta\cos\Theta)\Theta^{-3}$ with $\Theta = \sqrt{(\omega_1 c_1)^2 + (\omega_2 c_2)^2}$. The heat source has an elliptical base with a center at the origin, and two different elliptical radii are chosen to identify directions. The halfspace is translating with a sinusoidal Péclet number, $Pe_1(t) = 10\sin(2\pi t/0.6)$ (Fig. 7).

The dimensional heat source is defined as, $\overline{q} = \mu_f p(r)\overline{V}_1(t)$, a function of both position and time, where the constant frictional coefficient, μ_f, is 0.1. Therefore, $q = \sin(2\pi t/0.6)\sqrt{1-(x_1/c_1)^2-(x_2/c_2)^2}$. Both surface temperature rise and normal surface thermoelastic displacement of the halfspace are calculated in the region of $x_1 \in [-4, 4]$ and $x_2 \in [-3, 3]$ using Eqs. (6) and (14), and the results are plotted in Figs. 8 and 9, respectively. In these two figures, (a) through (h) correspond to the positions a through h on the sinusoidal Péclet-number curve shown in Fig. 7. The motion direction directly influences the contour spreading direction and the location of the maximum value, which is not at the origin again. Figures 8(e) and 9(e), which show the results after the motion direction is reversed, clearly indicating the residual fields of the responses from the previous motion.

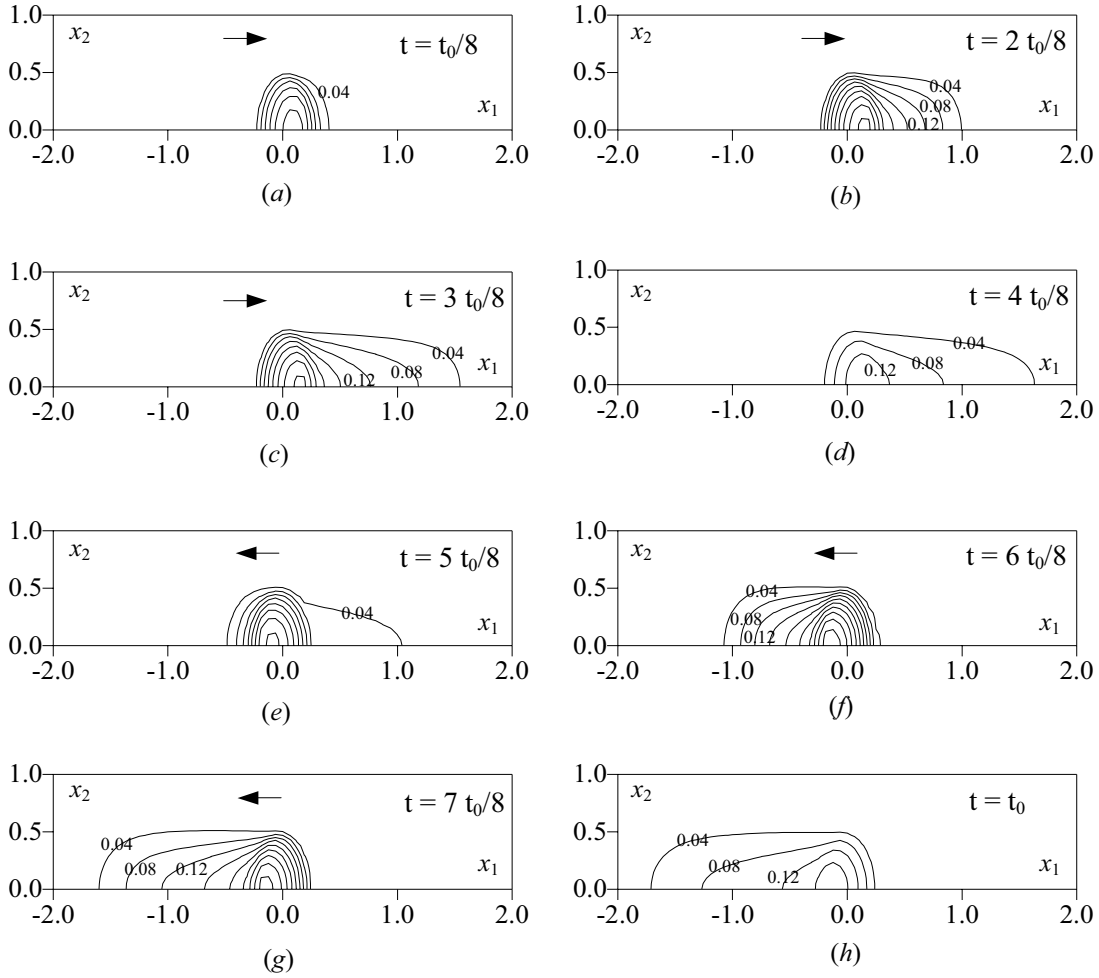

Figure 8 : Contours of the distributions of the surface temperature rise, $T(x_1, x_2, 0, t)$,on the surface of the reciprocating halfspace (Fig. 2(b)). Here, (a) through (h) are corresponding to positions 'a' through 'h' on the sinusoidal Péclet-number curve shown in Fig. 7.

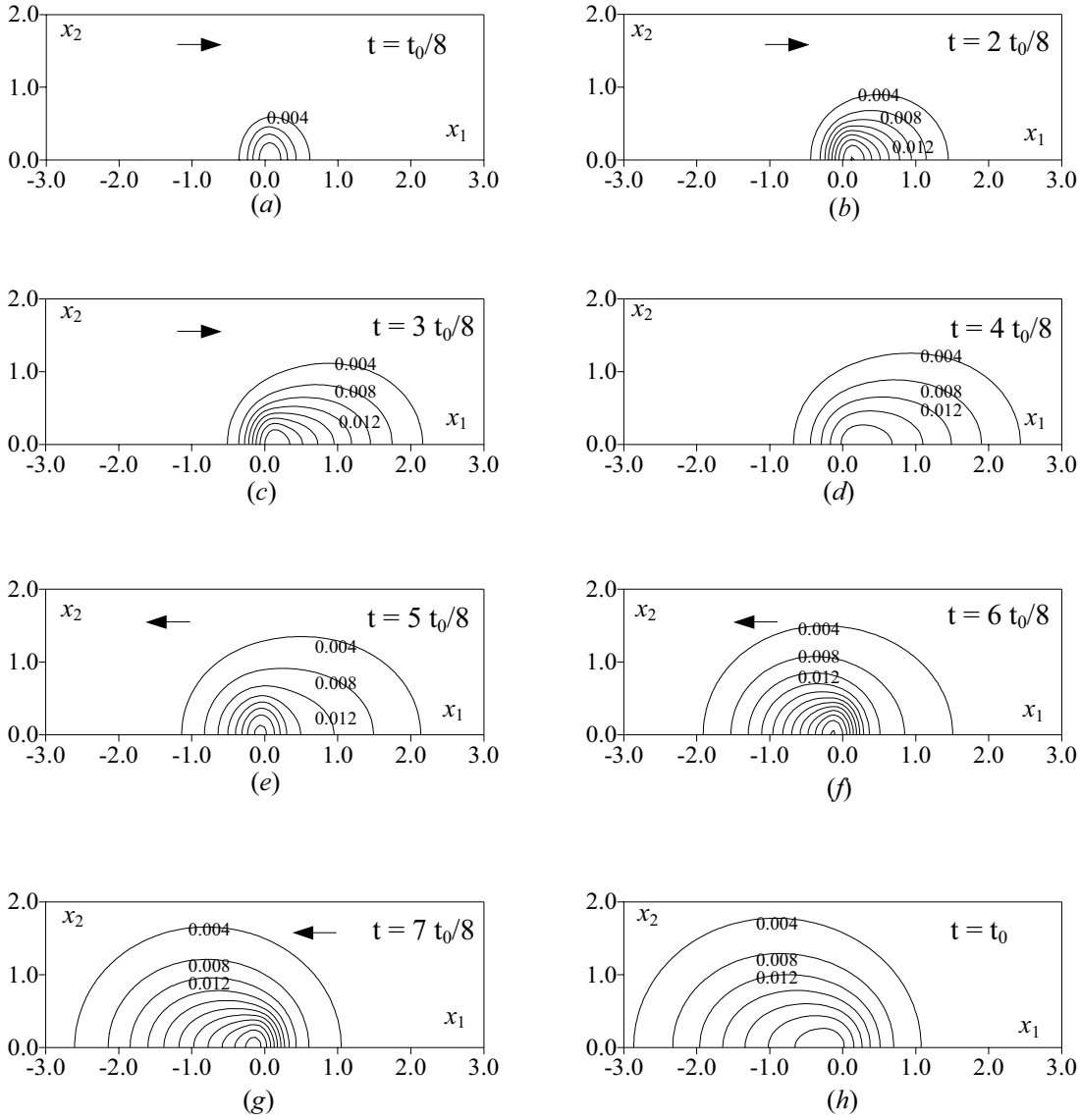

Figure 9 : Contours of the thermoelastic displacements, $-u_3(x_1, x_2, 0, t)$, of the surface reciprocating halfspace (Fig. 2(b)). Here, (a) through (h) are corresponding to positions 'a' through 'h' on the sinusoidal Péclet-number curve shown in Fig. 7.

The peak values in Figs. 8 - 9 oscillate because the heat source oscillates following the sinusoidal Péclet-number. The values are higher in the second half of the motion than in the first half of the motion due to the residual effects.

6.3 Circular Translation

When the halfspace is powered by two parallel cranks, it will perform a circular translation, as shown in Fig. 2 ($c1$). The velocities for all the points of the halfspace are the same at any given time. The coordinate system is fixed to the heat source, which is stationary. The trajectory of any point of the heat source on the surface of the halfspace should be a part of a circle whose radius is the length of the crank, which is unity for the current case. The initial velocities of the halfspace are $Pe_1(0) = 0$ and $Pe_2(0) = 10$. Due to the circular translation of the halfspace, the Péclet numbers are functions of time,

$$Pe_1(t) = Pe_2(0)\sin[-Pe_2(0)\,t] \tag{19}$$

$$Pe_2(t) = Pe_2(0)\cos[Pe_2(0)\,t] \tag{20}$$

This case could be interpreted equivalently by Fig. 2 ($c2$), as if the halfspace were stationary, and the heat source and the coordinate system were translating circularly. A heat source that corresponds to an identical Hertzian pressure distribution as in section 6.2 is applied. However, the dimensional heat source is time-independent, $\overline{q} = \mu_f p \overline{V}_2(0)$, where $\mu_f = 0.1$ and $\overline{V}_2(0)$ is the initial dimensional velocity ($Pe_2(0)\kappa/l$). Therefore, $q = \sqrt{1-(x_1/c_1)^2-(x_2/c_2)^2}$. The responses corresponding to four different times (Fig. 10(e)) in a region of $x_1 \in [-4,\ 4]$ and $x_2 \in [-4,\ 4]$ are analyzed with Eqs. (8) and (17) and are plotted in Figs. 10 - 11, respectively. Note that the x_2 axis is upward in Fig. 10. The arrows in Figs. 10 ($a-d$) and Figs. 11 ($a-d$) indicate the heated trajectory on the surface of the halfspace. Both responses spread in favor of the motion direction, and the tendency is more obvious in Fig. 10. At the given velocity and with the chosen radius of motion, the maximum temperatures, as marked in Fig. 10, are more sensitive to the alignment of the major axis of the heat-source base and the motion direction of the halfspace. Higher temperatures are found at $t = \pi/10$ and $t = \pi/5$, at which times the heat source has traveled one half and a full circle, respectively, where the major axis of the ellipse is along the motion direction of the heat source. Moreover, Fig. 11 obviously shows that the heat influence region for displacement is broader than that for temperature rise. When the halfspace travels a complete cycle, the outer contours look almost like circles, as shown in Fig. 11(d).

7 Conclusion

A novel set of frequency-domain formulations for the distribution of temperature rise and the normal surface thermoelastic displacement in a moving frictionally-heated elastic halfspace are derived by using the Carslaw and Jaeger results, the Seo-Mura results, and the Fourier transform. The velocity of the body can be an arbitrary function of time. General formulas are expressed in the form of time integrals, and important expressions for constant body motion velocities are given for the transient-instantaneous, transient-continuous, and steady-state cases. This theoretical development will enable the thermomechanical contact analysis for moving bodies by means of superposition of the results from this analysis with those from an isothermal elastic analysis of the same bodies under the excitation of non-zero tractions.

The thermoelastic responses, in terms of temperature rise and normal surface displacement, of the halfspace in configurations analogous to pin-on-disk experiments under pure translation, reciprocating translation, and circular translation are numerically simulated. Both the responses favor the direction of the body motion.

Acknowledgement: The authors would like to express their sincere gratitude to the support from US Office of Naval Research and National Science Foundation.

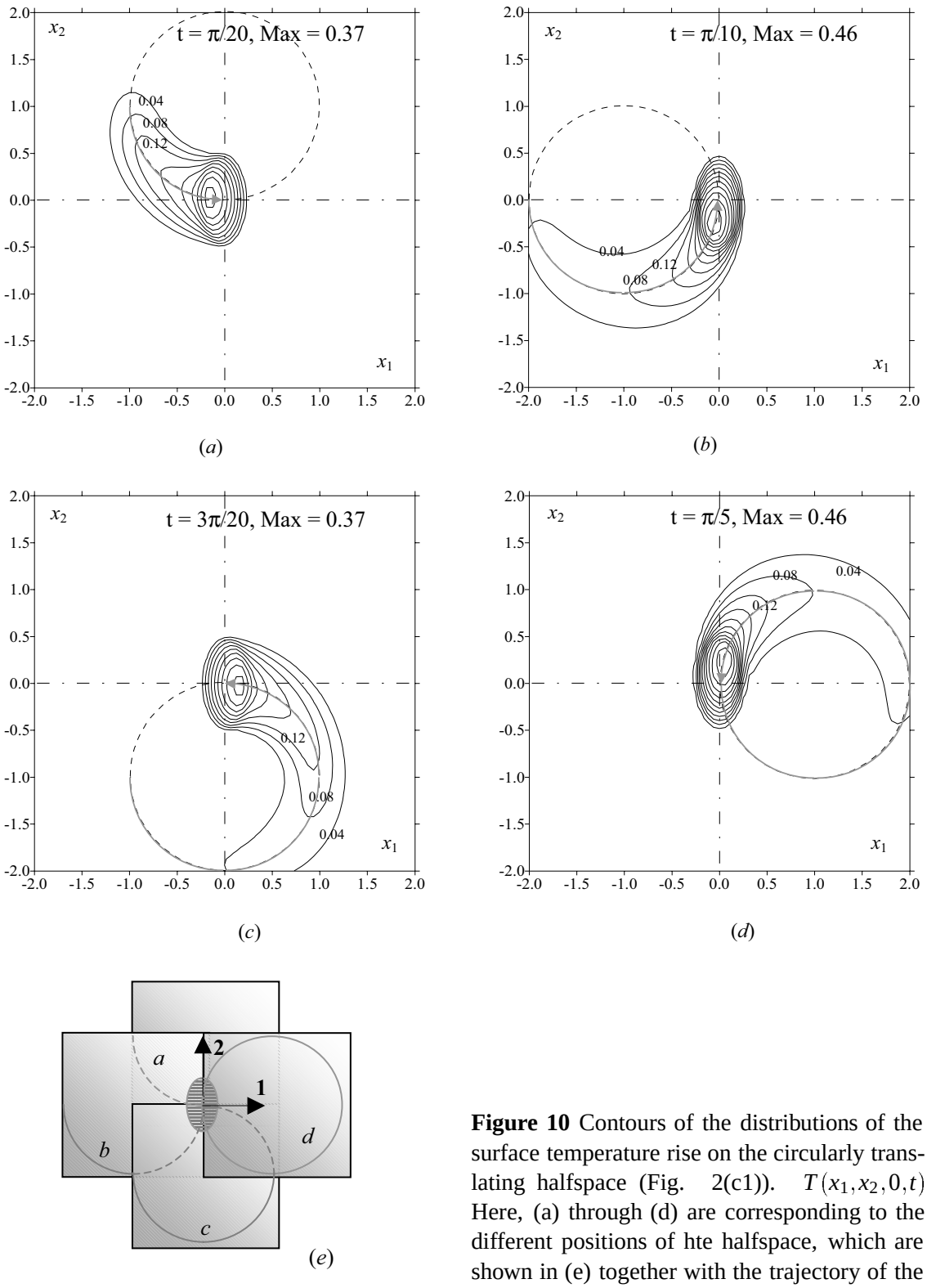

Figure 10 Contours of the distributions of the surface temperature rise on the circularly translating halfspace (Fig. 2(c1)). $T(x_1, x_2, 0, t)$ Here, (a) through (d) are corresponding to the different positions of hte halfspace, which are shown in (e) together with the trajectory of the heat source on the surface of the halfspace.

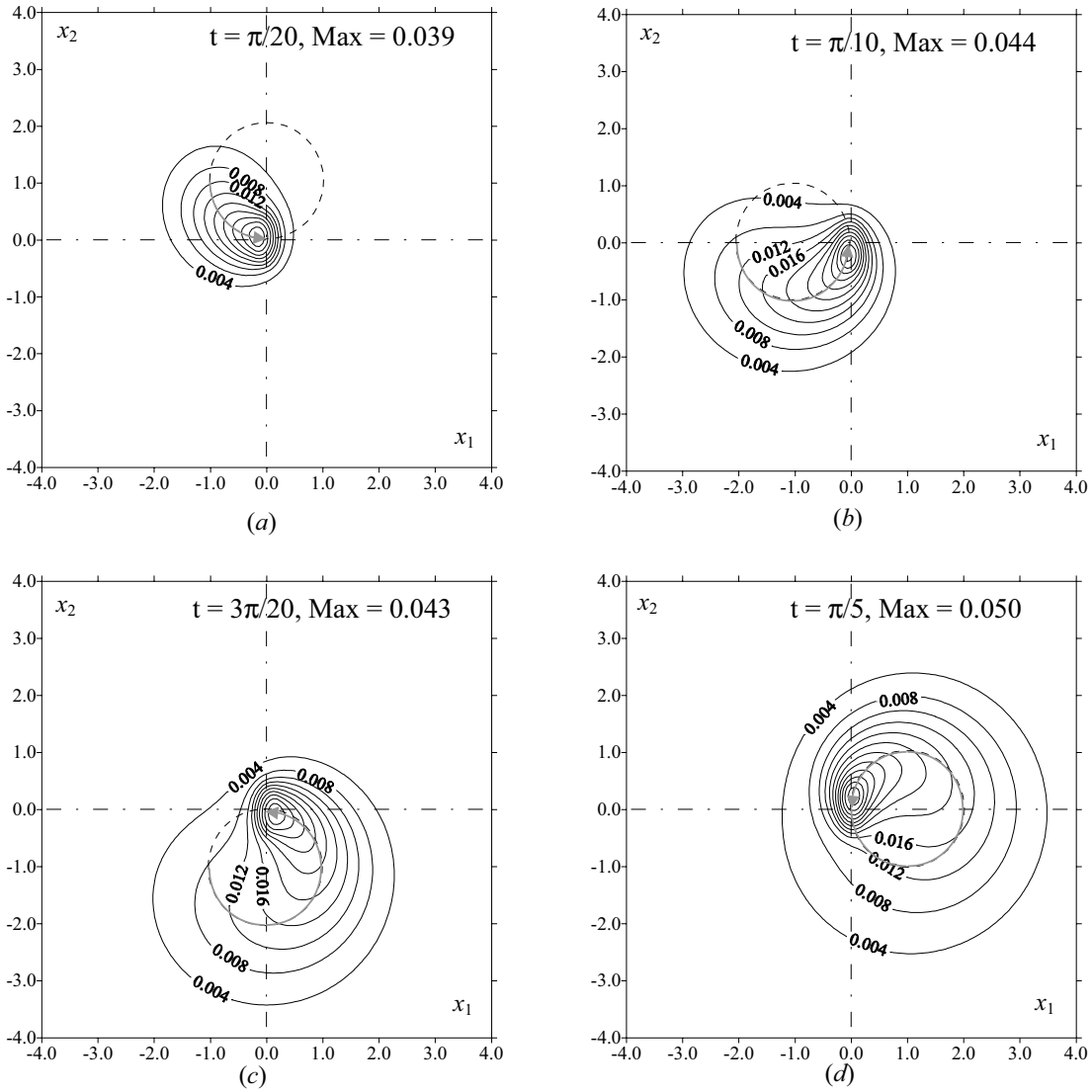

Figure 11 : Contours of the surface thermoelastic displacements, $-u_3(x_1, x_2, 0, t)$, of the circularly translating half-space (Fig. 2(c1)). Here, (a) through (d) are corresponding to the distributions of the temperature rise shown in Fig. 10.

Appendix A Fourier transforms

In the following equations, symbol '⇔' indicates that the left-hand side and the right-hand side are a Fourier transform pair.

1. The Fourier and inverse Fourier transforms [Morrison 1994]

$$F(x)=\frac{1}{2\pi}\int_{-\infty}^{+\infty}\tilde{F}(\omega_1)e^{+i\omega_1 x}d\omega_1 \quad \Leftrightarrow$$
$$\tilde{F}(\omega_1)=\int_{-\infty}^{+\infty}F(x)e^{-i\omega_1 x}dx \tag{A1}$$

where a single tilde $(\tilde{})$ implies a 1D Fourier transform.

2. The one-dimensional convolution theorem

$$F(x)=\int_{-\infty}^{+\infty}G(x')H(x-x')\,dx'=G(x)*H(x) \quad \Leftrightarrow$$
$$\tilde{F}(\omega_1)=\tilde{G}(\omega_1)\tilde{H}(\omega_1) \tag{A2}$$

where '*' implies a 1D convolution.

3. Shifting properties of the Fourier transform

Time-shift:

$$f(x-x_0) \quad \Leftrightarrow \quad \tilde{f}(\omega_1)\exp(-\mathrm{i}\omega_1 x_0) \tag{A3}$$

Frequency-shift (*modulation* in time domain):

$$f(x)\exp(\mathrm{i}\omega_0 x) \quad \Leftrightarrow \quad \tilde{f}(\omega_1-\omega_0) \tag{A4}$$

4. Fourier transform pairs ($t\geq 0$, $R=\sqrt{x_1^2+x_2^2+x_3^2}$, $x_3>0$)

$$G^T(\vec{x},t)=e^{-R^2/(4t)}/4(\pi t)^{3/2}\Leftrightarrow$$

$$\tilde{\tilde{G}}^T(\omega_1,\omega_2,x_3,t)=(\pi t)^{-1/2}e^{-\frac{x_3^2}{4t}-tw^2} \tag{A5}$$

$$G_3^{\mathrm{TE}}(\vec{x})=\frac{-x_3}{\pi R^3} \quad \Leftrightarrow \quad \tilde{\tilde{G}}_3^{\mathrm{TE}}(\omega_1,\omega_2,x_3)=-2e^{-x_3 w} \tag{A6}$$

$$f(t)=\mathrm{erfc}(w\sqrt{t})\Leftrightarrow\tilde{f}(\omega_t)=\frac{1}{\sqrt{w^2+\mathrm{i}\omega_t}\,(\sqrt{w^2+\mathrm{i}\omega_t}+w)} \tag{A7}$$

$$\exp(-\frac{x_3^2}{4t}-tw'^2)/\sqrt{\pi t}\Leftrightarrow$$

$$\exp\left(-x_3\sqrt{w'^2+\mathrm{i}\omega_t}\right)/\sqrt{w'^2+\mathrm{i}\omega_t} \tag{A8}$$

Appendix B Special function, $\varpi(z)$ [Abramowitz and Stegun, 1964]

The special function $\varpi(z)$ is defined as $\varpi(z)=\exp(-z^2)\,\mathrm{erfc}(-\mathrm{i}z) = -\mathrm{i}\exp(-z^2)\frac{2}{\sqrt{\pi}}\int_z^{\infty}\exp(t^2)\,dt$, where variable z is complex. Thus, $\mathrm{erfc}(z)=\varpi(\mathrm{i}z)\exp(-z^2)$ and $\mathrm{erf}(z)=1-\varpi(\mathrm{i}z)\exp(-z^2)$, and $z=x+\mathrm{i}y$ (x and y are real variables). For large x and y, function $\varpi(z)$ can be calculated by following expressions,

$$\varpi(z)=iz[0.4613135/(z^2-0.1901635)$$
$$+0.09999216/(z^2-1.7844927)$$
$$+0.002883894/(z^2-5.5253437)]+\eta_1(z),$$
$$|\eta_1(z)|<2\times 10^{-6},\ x>3.9 \text{ or } y>3 \tag{B1}$$

$$\varpi(z)=iz[0.5124242/(z^2-0.2752551)$$
$$+0.05176536/(z^2-2.724745)]+\eta_2(z),$$
$$|\eta_2(z)|<10^{-6},\ x>6 \text{ or } y>6, \tag{B2}$$

References

Abramowitz, M. and Stegun, I.A., (1964): Handbook of Mathematical Functions with Formulas, Graphs, and Mathematical Tables, National Bureau of Standards, Applied Mathematics Series (55).

Azarkhin, A. and Barber, J.R., (1987): Transient Contact of Two Sliding Half-Planes With Wear, *ASME Journal of Tribology*, **109**, pp. 598-603.

Barber, J.R., (1969): Thermoelastic Instabilities in the sliding of conforming Solids, *Proceedings of The Royal Society of London*, **A312**, pp.381-394.

Barber, J.R., (1972): Distortion of the Semi-infinite Solid Due to Transient Surface Heating, *International Journal of Mechanical Sciences*, **14**, pp. 377-393.

Barber, J.R. and Martin-Moran, C.J., (1982) Green's Function for Transient Thermoelastic Contact Problems for the Half-Plane, *Wear*, **79**, pp. 11-19.

Barber, J.R., (1984): Thermoelastic Displacements and Stresses Due to a Heat-Source Moving Over the Surface of a Half Plane, *ASME Journal of Applied Mechanics*, **51** (3), pp. 636-640.

Barber, J. R. (1987): Thermoelastic Distortion of the Half-space, *Journal of Thermal Stresses*. **10**, pp. 221-228.

Bryant, M., (1988) Thermoelastic Solutions for Thermal Distributions Moving Over Half Space Surfaces and Application to the Moving Heat Source, *ASME Journal of Applied Mechanics*, **55**, pp. 87-92.

Carslaw, H.S. and Jaeger, J.C., (1959): *Conduction of Heat in Solids*, Oxford University Press, London.

Dow, T.A. and Burton, R.A., (1972) Thermoelastic Instabilities in the Absence of Wear, *Wear*, **19**, pp.315-328

Gao J. Q., Lee, S. C., Ai, X. L., and Nixon, H., (2000): An FFT-Based Transient Flash Temperature Model for General Three-Dimensional Rough Surface Contacts, *ASME Journal of Tribology*, **122**, pp.519-523.

Huang, J.H. and Ju, F.D., (1985): Thermomechanical Cracking Due to Moving Frictional Loads, *Wear*, **102**, pp. 81-104.

Johnson, K. L., (1996): *Contact Mechanics*, Cambridge University Press.

Ju, F.D. and Chen, T.Y., (1984): Thermomechanical Cracking in Layered Media from Moving Friction Load, *ASME Journal of Tribology*, **106,** pp.513-518.

Ju, Y. and Farris, T.N., (1997): FFT Thermoelastic Solution for Moving Heat Sources, *ASME Journal of Tribology*, **119**, pp.156-162.

Leroy, J.M., Floquet, A., and Villechaise, B., (1989): Thermomechanical Behavior of Multilayered Media: Theory, *ASME Journal of Tribology*, **112,** pp.317-323.

Leroy, J.M., Floquet, A., and Villechaise, B., (1990): Thermomechanical Behavior of Multilayered Media: Results, *ASME Journal of Tribology*, **111,** pp.538-544.

Ling, F.F., and Mow, V.C., (1965) Surface Displacement of a Convective Elastic Half-Space under an Arbitrarily Distributed Fast-Moving Heat Source, *Journal of Basic Engineering*, pp.729-734.

Ling, F. F., (1973): *Surface Mechanics*, John Wiley & Sons, New York.

Liu, G. and Wang, Q., (2000): Thermoelastic Asperity Contacts, Frictional Shear, and Parameter Correlations, *ASME Journal of Tribology*, **122**, pp.300-307.

Liu, S.B., Wang, Q., and Liu, G., (2000): A Versatile Method of Discrete Convolution and FFT (DC-FFT) for Contact Analyses, *Wear*, **243**, No. 1-2, pp.101-110.

Liu, S.B., Rodgers, M., Wang, Q., and Keer, L., (2001): A Fast and Effective Method For Transient Thermoelastic Displacement Analyses, *ASME Journal of Tribology*, **123**, pp. 479-485.

Liu, S.B. and Wang, Q., (2001): A Three-Dimensional Thermomechanical Model of Contact Between Non-Conforming Rough Surfaces, *ASME Journal of Tribology*, **123**, pp. 17-26.

Liu, S.B. and Wang, Q., (2002): Studying Contact Stress Fields Caused by Surface Tractions with a Discrete Convolution and Fast Fourier Transform Algorithm, *ASME Journal of Tribology,* **124**, pp. 36-45.

Mindlin, R.D., (1953): Force at a Point in the Interior of a Semi-infinite Solid, Proc. The First Midwestern Conf. on Solid Mechanics, pp. 55-59.

Morrison N., (1994): *Introduction to Fourier Analysis*, John Wiley and Sons, Inc.

Mow, V.C. and Cheng, H.S., (1967): Thermal Stresses in an Elastic Half-space Associated with an Arbitrary Distributed Moving Heat Source, *Journal of Applied Mathematics and Physics* (ZAMP), **18**, pp.500-507.

Press, W.H., Teukolsky, S.A., Vetterling, W.T., and Flannery, B.P., (1992): *Numerical Recipes in Fortran 77-The Art of Scientific Computing*, (second edition), Cambridge University Press, Cambridge, Chaps. 12, 13.

Qiu, L., Cheng, H.S., (1998): Temperature Rise Simulation of Three-dimensional Rough Surfaces in Mixed Lubricated Contact, *ASME Journal of Tribology*, **120**, pp.310-318.

Seo, K. and Mura, T., (1979): The Elastic Field in a Half Space Due to Ellipsoidal Inclusions with Uniform Dilatational Eigenstrains, *ASME Journal of Applied Mechanics*, **46**, pp.568-572.

Sneddon, I. N., (1951): *Fourier Transforms*, New York, McGraw Hill Book Company.

Tian, X. and Kennedy, F. E., (1994): Maximum and Average Flash Temperatures in Sliding Contacts, *ASME Journal of Tribology*, **116**, pp.167-173.

Ting, B.Y. and Winer, W.O., (1989) Frictional-Induced Thermal Influences in Elastic Contact Between Spherical Asperities, *ASME Journal of Tribology*, **111**, pp.315-322.

Wang, Q. and Liu, G., (1999+: A Thermoelastic Asperity Contact Model Considering Steady-State Heat Transfer, *STLE Tribology Transactions*, **42** (4), pp.763-770.

Yevtushenko, A. A. and Kovalenko, Y. V., (1995a): The Interaction of Frictional Heating and Wear at a Transient Sliding Contact, *Journal of Applied Mathematics and Mechanics*, **59**(3), pp. 459-466.

Yevtushenko, A.A. and Kulchytsky-Zhyhailo, R.D., (1995b): Axisymmetrical Transient Contact Problem for Sliding Bodies with Heat Generation, *International Journal of Solids and Structure*, **32** (16), pp. 2369-2376.

Yi, Y.B., Du, S.Q., Barber JR, and Fash, J.W., (1999): Effect of Geometry on Thermoelastic Instability in Disk Brakes and Clutches, *ASME Journal of Tribology*, **121** (4), pp. 661-666.